Proceedings Paper:
Ball, E.A. orcid.org/0000-0002-6283-5949 (2021) Investigation into series-fed microstrip patch arrays at 26 GHz, 28 GHz and 48 GHz – design, simulation and prototype tests. In: 2021 IEEE Texas Symposium on Wireless and Microwave Circuits and Systems (WMCS). 2021 IEEE Texas Symposium on Wireless and Microwave Circuits and Systems, 18-20 May 2021, Waco, TX, USA (Virtual conference). IEEE (Institute of Electrical and Electronics Engineers) . ISBN 9781665431392

https://doi.org/10.1109/WMCS52222.2021.9493271

Investigation into Series-Fed Microstrip Patch Arrays at 26 GHz, 28 GHz and 48 GHz – Design, Simulation and Prototype Tests

Edward A. Ball
Communications Research Group, The University of Sheffield, UK
e.a.ball@sheffield.ac.uk

***Abstract*—This paper investigates the design and evaluation of a set of 9 element, series-fed, patch arrays. A simple design approach and formulas are presented. This is followed by EM simulation results and lab measurement results for a set of prototypes operating over a range of frequencies relevant to millimeter wave (mmWave) systems. The simulation results based on the calculated array dimensions show good characteristics. The measured gains and radiation patterns agree well with the simulation results. Overall, the usefulness of the design strategy for application to antennas in the mmWave band is confirmed.**

***Index Terms*—Antenna arrays, microstrip antenna arrays, patch antennas, millimeter wave measurements.**

I. Introduction

The patch antenna is a very popular and low-cost antenna type. Its design is well understood and widely employed. However, its use in forming arrays can be challenging, due to the requirement to taper the elements to achieve sidelobe level (SLL) control and the need for mechanisms to provide phase shift between the elements to form a beam.

One compact array design format uses the series-fed array of microstrip patches [1] – [5]. This is very space efficient since it does not require parallel corporate feed networks to supply the patches, which would consume additional board space. However, this class of array has been reported to have limited operational bandwidth, when compared to a parallel feed array [5].

The tapering of the element widths in the array offers a mechanism to shape the beam profile [6] – [9] and control SLL. The power feeding mechanisms to the patches can be implemented by wide variety of approaches [5], [10] – [11]. In this paper a simple transmission line is used to interconnect the patches. The mutual coupling between the patches can also be an issue, requiring EM simulation to fully characterize its effect.

There is now much research and commercial interest in systems operating at circa 28 GHz and above. Future IoT, communications systems and other novel applications will benefit from a low-cost antenna design that offers useful gain. The series-fed array is a possible candidate for such systems and has triggered the research in this paper.

In this paper a design strategy for a series-fed array of patches is described, using transmission line theory. Then, EM simulation results from Keysight ADS are presented. Finally, measured lab results for the arrays realized on Rogers 4003C substrate are reported. The contributions of this paper are: 1) presentation of a simple and intuitive approach to series-fed array design, 2) PCB evaluation of the technique at mmWave frequencies.

II. Design Strategy

The general concept and architecture of the series-fed array investigated is shown in Fig. 1. In this paper it consists of 9 elements that have symmetrical dimensions about the centre element (i.e. element 1 is the same as element 9, element 8 is the same as element 2, etc).

The starting point for the design of the array is the design of the center element in the array: element 5. This is designed following well-known and standard techniques for a single resonant patch element, such as [12] which defines width and length. At this point, the length and width of what will become the centre element are known. Following the approach in [12] the input impedance of the single patch is also then known. To ease the matching within the array, the length Ln (n = 1...9) of a patch can be scaled by a *small* amount to make the input impedance of each patch at its edge purely real, without significantly changing its resonant frequency. The impedance seen at the edge of a patch is commonly in the range 200 – 300 ohms [12], [15].

The next step is to calculate the width Wn of all other patches in the array. This is done by applying a desired aperture scaling to achieve a desired SLL. In this design, a Dolph-Chebyshev weighting was chosen, with 20 dB target SLL, though other weighting functions could have been used. The resulting Dolph-Chebyshev weights are shown in TABLE I, noting the symmetry about the centre element.

TABLE I
Dolph-Chebyshev 9 Element Weights

D1, D9	**D2, D8**	**D3, D7**	**D4, D6**	**D5**
0.601	0.615	0.812	0.950	1.0

978-1-6654-0309-2/21/$31.00 ©2021 IEEE

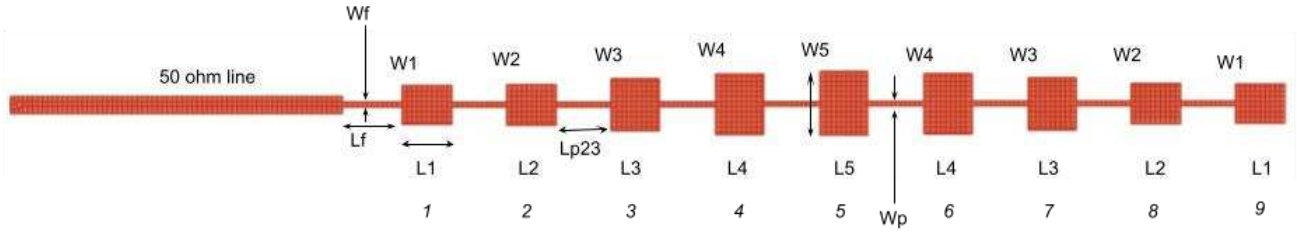

Fig. 1. Series-fed array structure.

To implement the Dolph-Chebyshev taper, the element weight values *Dn* are multiplied by the width of the initial (centre) element- resulting in a set of elements with tapered widths *Wn*, as shown in Fig. 1.

All the patches should then have their lengths adjusted *very slightly*, to ensure each patch input impedance is real-only [12]. The set of patch dimensions are thus known. To keep the design simple, inset feed lines were not used.

The spacing between the elements defines the beam pointing angle, via the array factor. The array can be considered as an array of point sources, fed sequentially on a transmission line. If the effective element spacing is 1 wavelength in the substrate, λ_g, then the resulting beam will be normal to the PCB with no grating lobes. The effective element spacing is the electrical distance between the *centers* of adjacent patches. As the lengths of each patch may be slightly different, as discussed above, the required length of the interconnecting tracks *Lpn,n+1* may also be different. However, in general *Lpn,n+1* will be close to $\frac{\lambda_g}{2}$. The design procedure should now continue leftwards (moving towards patch 1 and the input port) starting from patch element 9. To calculate the length of interconnecting tracks, the electrical length of each patch must be known, which requires an accurate model for the effective dielectric permittivity ε_{ref}, with [13] and [14] providing accurate models at mmWave. The microstrip patch electrical length is longer than the physical length, due to its edge effects [12]. The length of the interconnecting track is thus the length required to result in 1 λ_g spacing as measured from the centre of patch 8 to patch 9 or, more generally, patch *n* to patch *n* + 1. The impedance presented by patch 9 to the right-hand side (RHS) of patch 8 can then be evaluated using (1) where Z_n is the input impedance at the edge of patch 9, $Z0_{mn}$ is the characteristic impedance of the interconnecting line between patches *m* and *n,* of length Lp_{mn} (Lp_{89} between patches 8 and 9), and $\beta = \frac{2\pi}{\lambda_g}$.

$$Zin\_m\_RHS = Z0_{mn}\left(\frac{Z_n + jZ0_{mn}.tan(\beta.Lp_{mn})}{Z0_{mn} + jZ_n.tan(\beta.Lp_{mn})}\right) \quad (1)$$

The interconnecting line impedance $Z0_{mn}$ can be chosen to be close to the patch input impedance. The impedance presented to the RHS of patch 8 is then further transformed by patch 8 acting as a transmission line, with its own characteristic impedance $Z0p_8$ (different to $Z0_{mn}$) and electrical length Lp_8. The resulting impedance seen on the left-hand side (LHS) of patch 8, due to it acting as a simple transmission line, is then found by applying (2).

$$Zin\_m\_LHS = Z0p_m\left(\frac{Zin\_m\_RHS + jZ0p_m.tan(\beta.Lp_m)}{Z0p_m + jZin\_m\_RHS.tan(\beta Lp_m)}\right) \quad (2)$$

Let the impedance due to patch 8 acting just as a simple antenna (ignoring attached lines) be ZAp_8, or more generally ZAp_m. The imaginary part of ZAp_m can be made close to zero ohms, as described earlier. An example of the real part of ZAp_m for each element in a 26 GHz array is shown in Fig. 2a.

The composite impedance seen on the LHS of patch 8 can be evaluated as the parallel combination of ZAp_m and *Zin_m_LHS*, using (3) (where *m* = 8 for patch 8).

$$Zin\_m = \frac{Zin\_m\_LHS.ZAp_m}{Zin\_m\_LHS + ZAp_m} \quad (3)$$

This process of calculating the composite impedance then continues leftwards, through each patch, until the impedance on the left-hand side of patch 1 is known. The array input impedance should then be predominantly real.

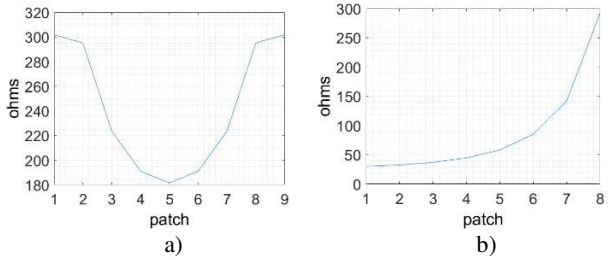

Fig. 2. Real part of impedances in 26 GHz array: a) individual patch input impedance ZAp_m, b) *Zin_m* seen on LHS of patches.

TABLE II
TRIAL ARRAY PATCH PHYSICAL DIMENSIONS

Antenna	***L1, L9* (mm)**	***W1, W9* (mm)**	***L2, L8* (mm)**	***W2, W8* (mm)**	***L3, L7* (mm)**	***W3, W7* (mm)**	***L4, L6* (mm)**	***W4, W6* (mm)**	***L5* (mm)**	***W5* (mm)**
26 GHz	3.0	2.3	3.0	2.4	2.9	3.1	2.9	3.6	2.9	3.8
28 GHz	2.8	2.1	2.8	2.2	2.7	2.9	2.7	3.4	2.7	3.6
48 GHz	1.6	1.2	1.6	1.3	1.6	1.7	1.6	2.0	1.6	2.1

TABLE III
TRIAL ARRAY PATCH INTERCONNECTING LINE PHYSICAL DIMENSIONS

Antenna	***Wf* (mm)**	***Lf* (mm)**	***Wp* (mm)**	***Lp12, Lp89* (mm)**	***Lp23, Lp78* (mm)**	***Lp34, Lp67* (mm)**	***Lp45, Lp56* (mm)**
26 GHz	0.3	3.6	0.3	3.3	3.3	3.4	3.4
28 GHz	0.3	3.6	0.3	3.0	3.0	3.1	3.1
48 GHz	0.4	2.4	0.3	1.8	1.8	1.8	1.8

Fig. 2b shows the real part of *Zin_m* at each patch in a 26 GHz array. A quarter wavelength transformer with dimensions *Lf*, *Wf* can then be used to convert the array input impedance to 50 ohms. For simplicity, thin interconnecting track width *Wp*, achieving a $Z0_{mn}$ of 100 ohms, was used for all arrays. This ensures the track is distinct from the patches, given their small size, with an impedance close to the patch. It may be possible to use an inset feed to achieve a 50 ohm match to patch 1, though care would be needed to ensure it does not adversely affect the radiation from patch 1.

The above outlined approach has been used to design 9 element arrays at 26 GHz, 28 GHz and 48 GHz, with final dimensions provided in TABLE II and TABLE III. A trial dual-array at 28 GHz was also simulated, using two identical 28 GHz arrays spaced by λ_g. A corporate feed power divider supplies the two 28 GHz arrays. The dual-array concept shown in Fig. 3.

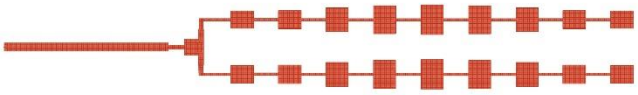

Fig. 3. The dual 28GHz array with corporate feed.

III. RESULTS

Results are now presented from EM simulations and a subsequent prototype build of the antenna designs, on Rogers R4003C substrate (thickness *h* of 0.5mm, relative permeability ε_r of 3.55 and tan delta of 0.0027).

A. EM Simulations

Keysight ADS was used to EM simulate the 4 different arrays. The dimensions for the patches and lines were used directly as calculated using the previously outlined technique. The only modification found necessary was a small reduction in the length of the interconnecting lines by a factor of 1.1, to ensure the beam was pointed normal to the PCB (otherwise a beam error of circa 10 degrees was observed).

Fig. 4a shows the coordinate systems. Fig. 4b shows an example 3D EM gain plot for the 26 GHz array. Fig. 5 – Fig. 8 show example EM simulation patterns of the 4 concept antennas, all showing a prominent beam normal to the PCB as expected.

From [15], the impedance fractional bandwidth (BW) can be found for a return loss (RL) > 9.5 dB. Due to the patch geometry, the impedance fractional BW of the patches is narrowest at the centre patch (3% - 5%) and increases outwards with the patch element location.

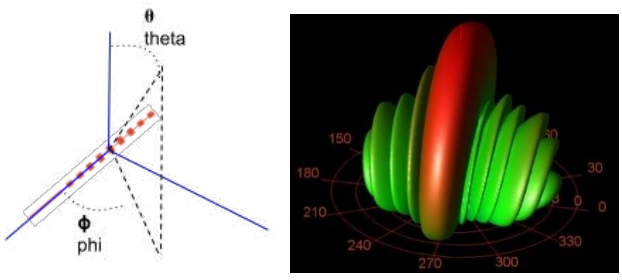

a) b)

Fig. 4. a) coordinate system, b) example 26 GHz array 3D EM simulation gain pattern.

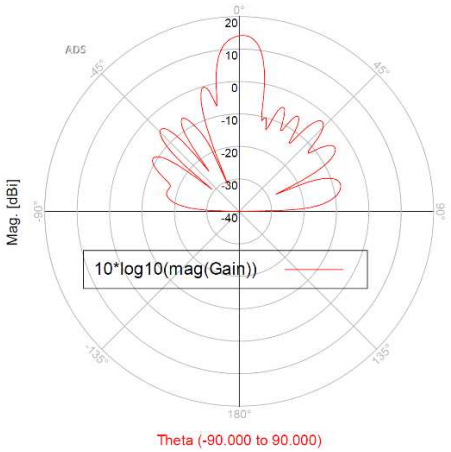

Fig. 5. 26 GHz array pattern simulation (phi = 0).

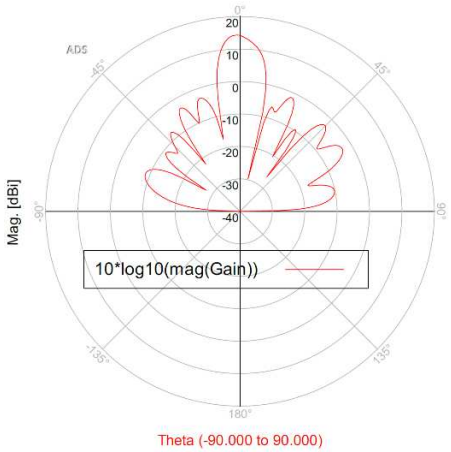

Fig. 6. 28 GHz array pattern simulation (phi = 0).

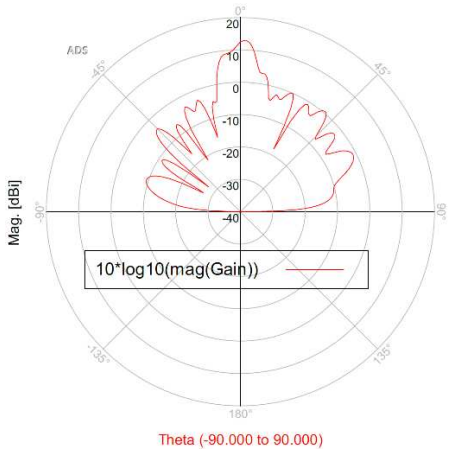

Fig. 7. 48 GHz array pattern simulation (phi = 0).

B. Prototype PCB Measurements

Fig. 9 shows the prototype PCB with the 4 arrays.

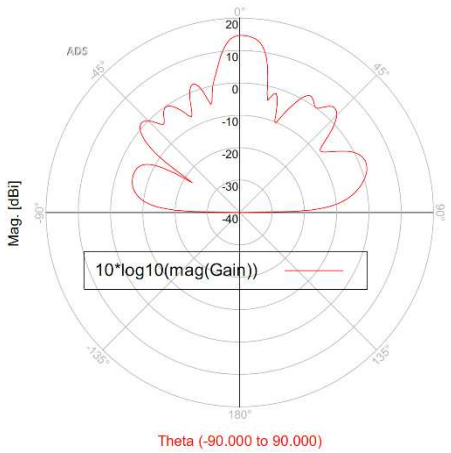

Fig. 8. 28 GHz dual-array pattern simulation (phi = 0).

The University of Sheffield Communications Research Group hosts the EPSRC mmWave Measurement Laboratory, which includes an advanced antenna measurement capability to 110 GHz [16], as shown in Fig. 10a. Fig. 10b shows the PCB array undergoing lab testing by the NSI-MI 700S-360 antenna measurement system. Using this facility, the patterns of the prototype PCB antennas have been measured and are presented below.

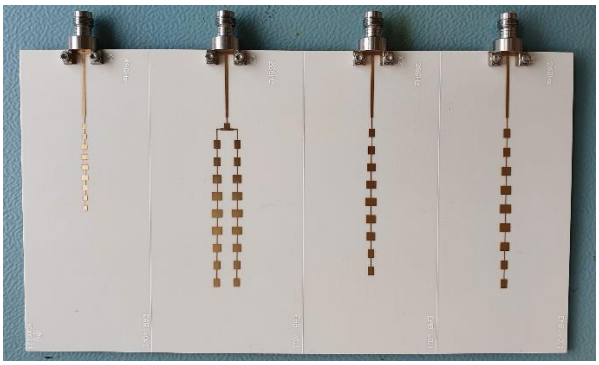

Fig. 9. Built prototype PCB showing all 4 array concepts.

a) b)

Fig. 10. a) EPSRC mmWave Measurement Laboratory, b) PCB arrays under test.

Fig. 11 – Fig. 16 show a selection of lab radiation pattern measurements for theta sweeps of -90 degrees to + 90 degrees, with phi set to 0 or 90 degrees as stated. The plots show both measured results and the EM simulation results, for comparison. All plots are normalized. Fig. 12 also shows the simulated array pattern when all patches are identical (i.e. no weighting applied) showing further degrading of SLL, as would be expected.

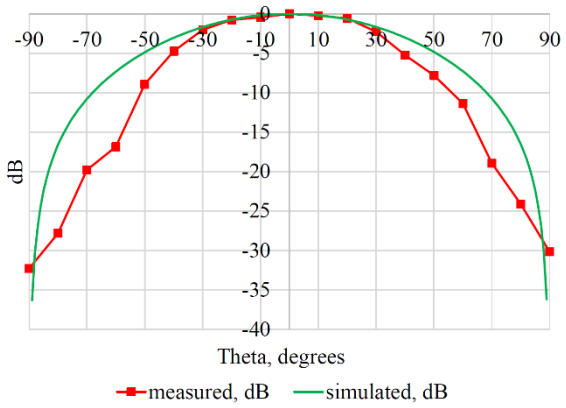

Fig. 11. Measured & simulation 26 GHz array pattern (phi = 90).

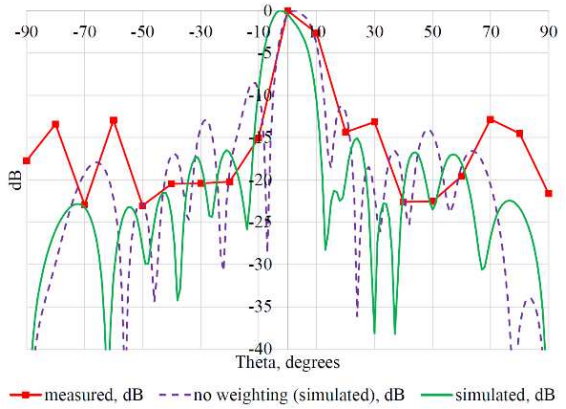

Fig. 12. Measured & simulation 28 GHz array pattern (phi = 0).

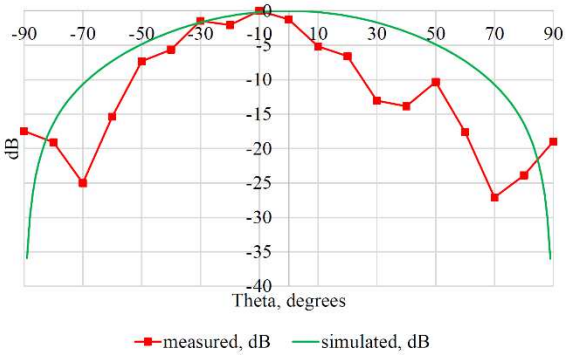

Fig. 13. Measured & simulation 28 GHz array pattern (phi = 90).

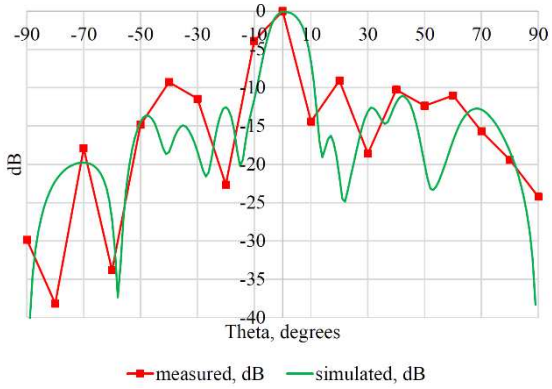

Fig. 14. Measured & simulation 28 GHz dual-array pattern (phi = 0).

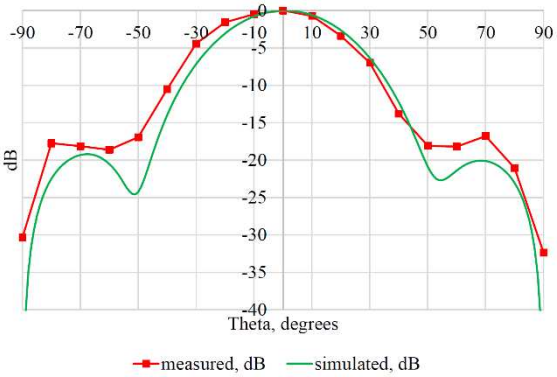

Fig. 15. Measured & simulation 28 GHz dual-array pattern (phi = 90).

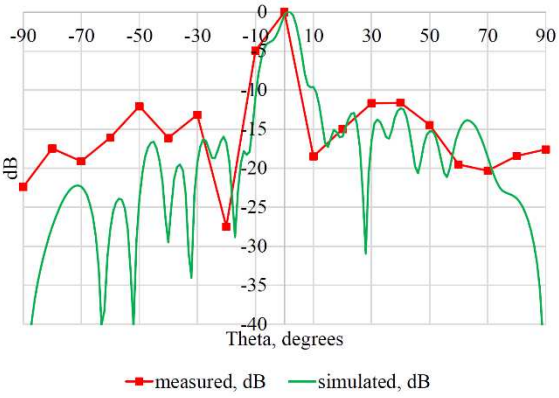

Fig. 16. Measured & simulation 48 GHz array pattern (phi = 0).

A summary of the lab and simulation measurements, and relevant published results, is presented in TABLE IV. As would be expected, the measured gains were lower than simulations, though with the 28 GHz arrays delivering closest to simulated gains. However, good isotropic gain is achieved, exceeding 8 dBi.

TABLE IV
MEASURED & SIMULATED ANTENNA ARRAY PERFORMANCE

Array	**RL** ***measured*** [simulated] **(dB)**	**RL BW (%)**	**Gain** ***Measured*** [simulated] **(dBi)**	**SLL** ***Measured*** [simulated] **(dB)**	***n***
26GHz	***20*** [23.0]	8.1	***9*** [14.2]	***-12*** [-14.4]	9
28GHz	***17*** [18.8]	5.0	***11*** [14.3]	***-13*** [-15.8]	9
48GHz	***9*** [14.5]	7.7	***8*** [13.0]	***-12*** [-13.0]	9
28GHz dual	***14*** [19.4]	5.0	***12*** [14.7]	***-9*** [-11.0]	9
[6]	18	2.8	-	-14	5
[9]	12	7.1	15.4	-11	10
[3]	25	2.0	16	-22	10
[8]	12.2	6.3	-	-23.8	16
[10]	***15***	19.6	***15.0***	***-20***	5

It was observed that the gain of the 28 GHz dual-array was only ~1 dB higher than the single array. Subsequent EM simulations of the corporate feed network have identified its loss to be 5.5 dB, thus explaining the negligible gain enhancement seen in the dual array. The observed reduction in gain for the single series-fed arrays could be due to radiated measurement uncertainty, PCB edge launch connector loss or further PCB losses.

A subsequent EM simulation assessing the mutual coupling between adjacent elements in the 28 GHz array identified a coupling of -20 dB. Since mutual coupling effects were not considered in the design strategy, it is suspected this has led to the limited SLL achieved.

IV. CONCLUSION

A simple approach to designing a set of 9 element series-fed patch antenna arrays is described and evaluated. The simulated and measured results confirm the validity of the approach and show good agreement. The arrays offer useful gain for practical low-cost mmWave applications on PCB. Further work is required to optimise SLL.

ACKNOWLEDGMENT

This work was in part supported by a UKRI Future Leaders Fellowship [grant number MR/T043164/1].

The author would like to thank Steve Marsden for performing laboratory radiated measurements.

REFERENCES

[1] Jones B, Chow F, and Seeto A, "The synthesis of shaped patterns with series fed microstrip patch arrays," *IEEE Trans. on Antennas and Prop.*, vol. 30, no. 6, pp. 1206–1212, Nov. 1982, doi: 10.1109/TAP.1982.1142963.

[2] S. Sengupta, D. R. Jackson, and S. A. Long, "A method for analyzing a linear series-fed rectangular microstrip antenna array," *IEEE Transactions on Antennas and Propagation*, vol. 63, no. 8, pp. 3731–3736, Aug. 2015, doi: 10.1109/TAP.2015.2436407.

[3] B. Jian, J. Yuan, and Q. Liu, "Procedure to design a series-fed microstrip patch antenna array for 77 GHz automotive radar," in *Proc. 2019 Cross Strait Quad-Regional Radio Science and Wireless Technology Conference (CSQRWC)*, 2019, pp. 1–2, doi: 10.1109/CSQRWC.2019.8799356.

[4] B. Singh, N. Sarwade, and K. P. Ray, "Compact series fed tapered antenna array using unequal rectangular microstrip antenna elements," *Microwave and Optical Technology Letters*, vol. 59, no. 8, pp. 1856–1861, Aug. 2017, doi: 10.1002/mop.30640.

[5] R. Garg, P. Bhartia, I. Bahl, and A. Ittipiboon, *Microstrip Antenna Design Handbook*, 1st Edition. Norwood: Artech House, 2001.

[6] T. Yuan, J. Y. Li, L. W. Li, L. Zhang, and M. S. Leong, "A novel series-fed taper antenna array design and analysis," in Proc. *Asia-Pacific Microwave Conference APMC*, 2005, vol. 4, doi: 10.1109/APMC.2005.1606890.

[7] T. Yuan, N. Yuan, and L. W. Li, "A novel series-fed taper antenna array design," *IEEE Antennas and Wireless Propagation Letters*, vol. 7, pp. 362–365, July 2008, doi: 10.1109/LAWP.2008.928487.

[8] B. Li, Y. Qiu, J. Zhang, Z. Zhou, and L. Sun, "W-band Series-fed Microstrip Patch Array with Optimization of Tapering Profile," Aug. 2020, doi: 10.1109/APCAP50217.2020.9246094.

[9] A. Omar, S. Al-Saif, M. A. Ashraf, and S. Alshebeili, "Design and analysis of millimeter wave series fed microstrip patch array for next generation wireless communication systems," in *Proc. 2016 17th International Symposium on Antenna Technology and Applied Electromagnetics (ANTEM)*, 2016, doi: 10.1109/ANTEM.2016.7550139.

[10] H. A. Diawuo, K. Anim, and Y. B. Jung, "Coupled-line proximity-coupled microstrip linear array antenna for millimetre-wave applications," *IET Microwaves, Antennas and Propagation*, vol. 14, no. 14, pp. 1886–1894, Nov. 2020, doi: 10.1049/iet-map.2020.0052.

[11] A. Aslam and F. A. Bhatti, "Improved design of linear microstrip patch antenna array," in *Proc. 2010 9th International Symposium on Antennas Propagation and EM Theory, ISAPE*, 2010, pp. 302–306, doi: 10.1109/ISAPE.2010.5696460.

[12] C. Balanis, "14.2 Rectangular patch," in *Antenna Theory*, Third Edition., Hoboken: Wiley Interscience, 2005, pp 816-823.

[13] T. C. Edwards and M. B. Steer, "Formulas for Accurate Static-TEM Design Calculations," in *Foundations of Interconnect and Microstrip Design*, Third Edition., Chichester: Wiley, 2000, pp. 92–93.

[14] T. C. Edward and M. B. Steer, "Expressions Suitable for Millimetre-Wave Design," *in Foundations of Interconnect and Microstrip Design*, Third Edition., Chichester: Wiley, 2000, pp. 124–127.

[15] Y. Huang and K. Boyle, "Popular Antennas," *in Antennas from Theory to Practice*, First Edition., Chichester: Wiley, 2008, pp. 187–188.

[16] University of Sheffield EPSRC mmWave Measurement Laboratory website. [Online]. Available: https://mmwave.group.shef.ac.uk/